

Crystal Plasticity Analysis of Dislocation Accumulation in ULSI Cells with Consideration of Temperature Dependence of the Lattice Friction Stress for Silicon

Michihiro Sato^{1, a}, Tetsuya Ohashi^{1, b}, Takuya Maruizumi² and Isao Kitagawa³

¹Department of Mechanical Engineering, Kitami Institute of Technology,
165 Koen-cho, Kitami, Hokkaido 090-8507 Japan

²Department of Electrical and Electronic Engineering, Musashi Institute of Technology,
1-28-1 Tamazutsumi, Setagaya-ku, Tokyo 158-8557, Japan

³Advanced Research Laboratory, Hitachi, Ltd.,
1-280 Higashi-koigakubo, Kokubunji, Tokyo 185-8601, Japan

^asato@newton.mech.kitami-it.ac.jp, ^bohashi@newton.mech.kitami-it.ac.jp

Keywords : ULSI, Dislocation, Crystal plasticity analysis, Finite element method

Abstract. Representative length scale of ULSI (Ultra Large Scale Integration) cells is going to be at a nano-meter order, and the atomic level defects, such as uneven oxide films or dislocation accumulation are becoming more and more important. Among these defects, dislocation accumulation is known to be caused by thermo-plastic deformation in silicon during the processes of device fabrication. In this study, we analyse such thermal stress, plastic slip deformation and accumulation of dislocations in STI (Shallow Trench Isolation) type ULSI devices when the temperature drops from the initial at 1000 to room temperature. For the analysis, we use a crystal plasticity analysis code CLP, assuming that lattice friction stress for the movement of dislocations is proportional to the hardness of silicon, which is known to have strong dependency on temperature. The results show that dislocations are generated between the temperature range from 880 to 800, and its maximum density is highly dependent on the lattice friction stress in the temperature range above 800. For example, the difference of 16 MPa in the lattice friction stress at 1000 caused increase in dislocation density more than ten times. It is concluded that control of lattice friction stress at high temperatures is one of the most promising way for the suppression of dislocation accumulation.

Introduction

In recent years, high-density memories and high-speed CPUs are usually realized by a reduction of the size of semiconductor cells in LSIs. Representative length scale of ULSI cells is going to be at a nano-meter order and the atomic level defects, such as uneven oxidation film or lattice defect generation etc., are becoming more and more important. Among them, dislocations which often appear near hetero-interfaces and accumulate in the electron channel have an enormous effect on the electronic state of the device, increase the signal delay and obstruct devices from normal operation. Therefore, the evaluation and control of dislocations are crucial not only for the design of cell structure but also for the design of process through which ULSI chips are produced. The periodic structure of the shallow trench isolation (STI) type ULSI cells are generally adopted as the latest semiconductor device structure. A lot of investigations have been made on this type of structure and dislocation accumulation is known to be caused by thermo-plastic deformation in silicon during the processes of device fabrication, but detailed aspects on dislocations and their density distribution in the cells are not fully understood. In this study, we analyse such thermal stress, plastic slip deformation and accumulation of dislocations in STI type ULSI devices when the temperature drops from 1000 to room temperature. For the analyses, we use a continuum mechanics based crystal plasticity analysis code CLP[1,2].

Model for numerical analysis

Fig. 1 (a) schematically shows the periodic structure of the STI type ULSI cells. One unit of the periodic structure is cut out and we employ it for the numerical analyses. Fig. 1 (b) shows the model used in the analyses. Dimensions of the model is typical for STI structure with the gate length 62 nm. The structure consists of the volumes ① to ④, as shown in Fig. 1 (b). Volumes ① to ③ corresponds to gate, source and drain electrodes, respectively, and for simplicity their materials are assumed to be SiO₂. Volume ④ represents the Si substrate. Crystal orientation of the model is also shown in Fig. 1 (b). The normal of Si substrate (the Y axis) corresponds to the [100] direction and trench direction of STI structure is parallel to the [01 $\bar{1}$] direction. Table 1 shows the material data [3,4] used for the analysis. We assume the deformation in the z direction is negligibly small because the dimension of the STI structure in the z direction is long enough compared to those in the x and the y direction. Then, in the numerical model, the nodes on the surfaces perpendicular to the z axis are constrained to displace in the z direction. Nodes on the surfaces which are perpendicular to the x axis are subjected to obey a periodic boundary condition in x direction. The models are divided into finite elements. The type of the elements is the composite element with eight nodes. The numbers of nodes and elements in a model is 10492 and 7560, respectively.

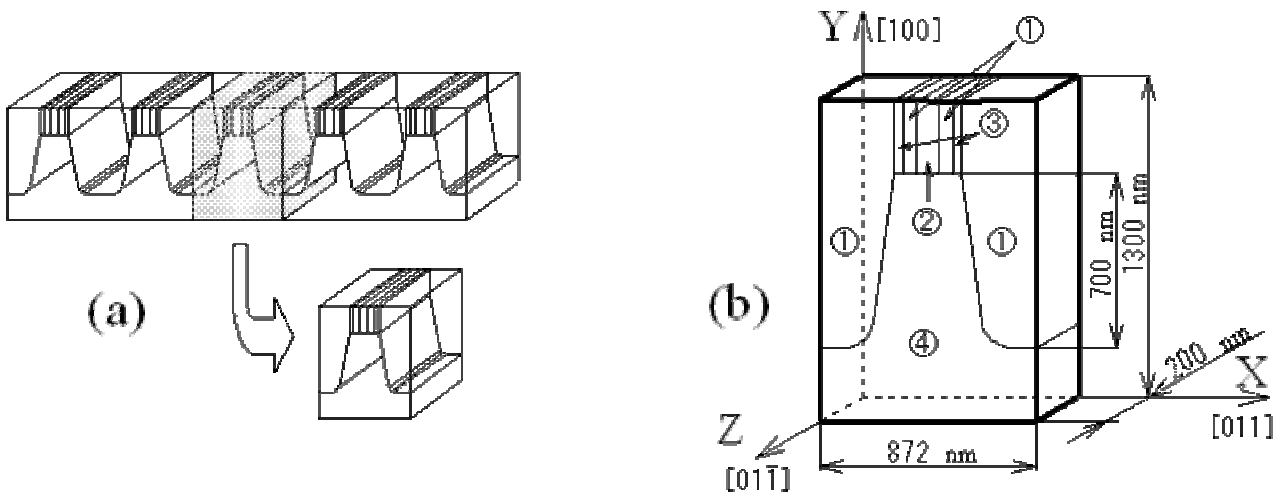


Fig. 1 (a) Schematic illustration of the periodic structure of the STI type ULSI cells.
 (b) Model employed for the crystal plasticity analysis.

Table 1 Material data used in the analyses [3,4].

	Elastic compliances [10 ⁻¹¹ m ² /N]			Thermal expansion coefficient [1/K]
Si	S ₁₁ =0.7685	S ₁₂ =-0.2139	S ₄₄ =1.2563	2.50 × 10 ⁻⁶
SiO ₂	S ₁₁ =1.3698	S ₁₂ =-0.2327	S ₄₄ =3.2051	0.35 × 10 ⁻⁶

Crystal plasticity analysis

The plastic slip occurs on {111} slip plane in <110> slip direction and there are 12 combinations of slip plane and slip direction, which define the 12 slip systems. Dislocations which accumulate after plastic slip are categorized into two kinds; statistically stored dislocations (SS dislocations) and geometrically necessary dislocations (GN dislocations). SS dislocations represent the ones which are trapped by randomly distributed implicit obstacles in the microstructure, and we do not

need to consider about them in this paper since the Si area is supposed to be perfect crystal before deformation. Accumulation of the geometrically necessary dislocations is studied in this paper. The geometrically necessary dislocations accompany to the spatial gradient of plastic shear strain on slip systems. Ashby introduced the one-dimensional concept of geometrically necessary dislocations as follows [5];

$$\rho_G \cdot \tilde{b} = -\frac{\partial \gamma}{\partial \xi} , \quad (1)$$

where, ρ_G denotes the density of the geometrically necessary dislocations. γ , \tilde{b} and ξ are the plastic shear strain, the magnitude of the Burgers vector, and the direction parallel to the slip direction on the slip plane, respectively. In three dimensional space, the densities of geometrically necessary dislocations are given for the edge and screw components [2];

$$\rho_{G,edge}^{(n)} \cdot \tilde{b} = -\frac{\partial \gamma^{(n)}}{\partial \xi^{(n)}} , \quad (2)$$

$$\rho_{G,screw}^{(n)} \cdot \tilde{b} = \frac{\partial \gamma^{(n)}}{\partial \zeta^{(n)}} , \quad (3)$$

where, superscript (n) denotes the slip system number. ξ is the direction perpendicular to the slip direction on the slip plane. Gradient of plastic shear strain in each element is calculated to evaluate density components $\rho_{G,edge}^{(n)}$ and $\rho_{G,screw}^{(n)}$. The norm of the two components gives the density of geometrically necessary dislocations [2];

$$\|\rho_G^{(n)}\| = \sqrt{(\rho_{G,edge}^{(n)})^2 + (\rho_{G,screw}^{(n)})^2} . \quad (4)$$

The CLP calculates the plastic slip deformation on 12 slip systems of $\{111\}\langle 110 \rangle$ in crystals and evaluates the plastic shear strains, stresses and the density distributions of geometrically necessary (GN) dislocations.

In this analysis, we assume that the critical resolved shear stress on slip system is given by the modified Bailey-Hirsch type relation [6];

$$\theta^{(n)} = \theta_0(T) + \sum_{m=1}^{12} \Omega^{(nm)} a \mu \tilde{b} \sqrt{\rho_s^{(m)}} , \quad (5)$$

Where, the first term of the right hand side of Eq. 5 gives the lattice friction stress and the second term denote the strain hardening. SS dislocations that have accumulated on the m th slip system contribute to the critical resolved shear stress of the n th system through the component $\Omega^{(nm)}$. There are 12×12 components in $\Omega^{(nm)}$ and their values are given by five independent parameters, which are defined by elementary processes of interaction between dislocations on slip systems n and m . For simplicity, we assume a sufficiently small value for a and exclude the effect of strain hardening. Therefore, the critical resolved shear stresses on slip systems are decided only by temperature and do not depend on deformation history. As far as we know, there is no experimental data of lattice friction stress. On the other hand, the hardness of silicon was experimentally obtained in the range from 24 to 800 (Table 2), where hardness values are normalized by the hardness at 800. It is known, in general, that plastic flow stress is proportional to the hardness of crystalline material. In this paper, we made five data sets P42, P38,

P34, P30 and P26 for the lattice friction stress for silicon (Table 3). One set of data denoted as P42 and shown in Table 3 is calculated in such a way that the lattice friction stress at 800 K is 42 MPa and vary with temperature in the same way the hardness values (Table 2) change. At temperature lower than 800 K, the lattice friction stress increases when the temperature drops, and the lattice friction stress at 24 K becomes 10.2 times larger than the value at 800 K. Similarly, lattice friction stress given by the data sets P38, P34, P30 and P26 are calculated from the hot hardness values shown in table 2, provided that lattice friction stresses at 800 K are 38, 34, 30, and 26 MPa, respectively. The value after the letter P of these data set names show the lattice friction stress at 800 K. We assume the lattice friction stress is constant at temperature range from 800 to 1000 K, because there is no data at this temperature range. Lattice friction stresses between the each temperature given in table 3 are obtained by liner interpolation.

Table 2 Hot hardness values for silicon [7].

Temperature [K]	24	100	200	400	600	800
Hot hardness value	10.2	9.8	9.3	5.6	2.6	1.0

Table 3 Data sets of lattice friction stress used in the analyses.

Temperature [K]	24	100	200	400	600	800	1000
Lattice friction stress for silicon [MPa]							
P42	428	412	391	235	109	42	42
P38	388	372	353	213	99	38	38
P34	347	333	316	190	88	34	34
P30	306	294	279	168	78	30	30
P26	265	255	242	146	68	26	26

Results and discussion

We define the total length of dislocations (tdl) on each slip systems by the following equation;

$$tdl^{(n)} = \sum_i \|\rho_G^{(n)}\| \times v_i, \quad (6)$$

where, ρ_G is the density norm of the geometrically necessary dislocations, v_i is the volume of element i , and superscript (n) denotes the slip system number, respectively. We discuss about growth of the dislocation accumulation in the device using this tdl .

Fig. 2 (a) and (b) show evolution of the tdl on $(111)[\bar{1}\bar{1}0]$ and $(11\bar{1})[\bar{1}\bar{1}0]$ slip systems, when the temperature drops from 1000 K to room temperature. When the lattice friction stress is given by P30 and P26, tdl on the $(111)[\bar{1}\bar{1}0]$ slip system starts to increase at 820 and 840 K respectively and these values converge at 800 K (Fig. 2(a)). When the lattice friction stress is given by P34, dislocation accumulate at 800 K but it does not show notable growth (Fig. 2(a)). Dislocation accumulation on $(111)[\bar{1}\bar{1}0]$ slip system does not take place when the lattice friction stress is given by P42 and P38. Fig. 2 (b) shows growth of tdl on the $(11\bar{1})[\bar{1}\bar{1}0]$ slip system. Dislocations begin to accumulate in the temperature range from 820 to 880 K, and these values

converge at 800 . Small difference in the lattice friction stress makes a significant change in the accumulation of dislocations. For example, difference in the lattice friction stress given by P26 and P34 is 8 MPa in the range from 1000 to 800 and the temperature at which dislocation start to accumulate differ 40 on the $(111)[\bar{1}\bar{1}0]$ slip system (Fig. 2(a)). Difference in the lattice friction stress given by P26 and P42 is 16 MPa. By this difference of 16 MPa, the temperature at which dislocation start to accumulate differ 60 on the $(11\bar{1})[\bar{1}\bar{1}0]$ slip system. While, the temperature at which dislocation accumulation converge is 800 for all cases irrespective of difference in the lattice friction stress at temperature range from 1000 to 800 . The final values of tdl on the $(111)[\bar{1}\bar{1}0]$ slip system are 3.0 nm for P26 case and 0.4 nm for P34 case (Fig. 2 (a)). So, the difference of 8 MPa in the lattice friction stress at high temperature caused increase of dislocation accumulation more than 7.5 times. Similarly, on the $(11\bar{1})[\bar{1}\bar{1}0]$ slip system shown in Fig.2 (b), the final values of $tdls$ are 85.3 nm for P26 case and 8.7 nm for P42 case. The difference of 16 MPa in the lattice friction stress at high temperature caused increase of dislocation accumulation more than 10 times. These facts show that the difference of less than 20 MPa in the lattice friction stress at the temperature range from 1000 to 800 makes significant changes in dislocation accumulation in ULSI cells.

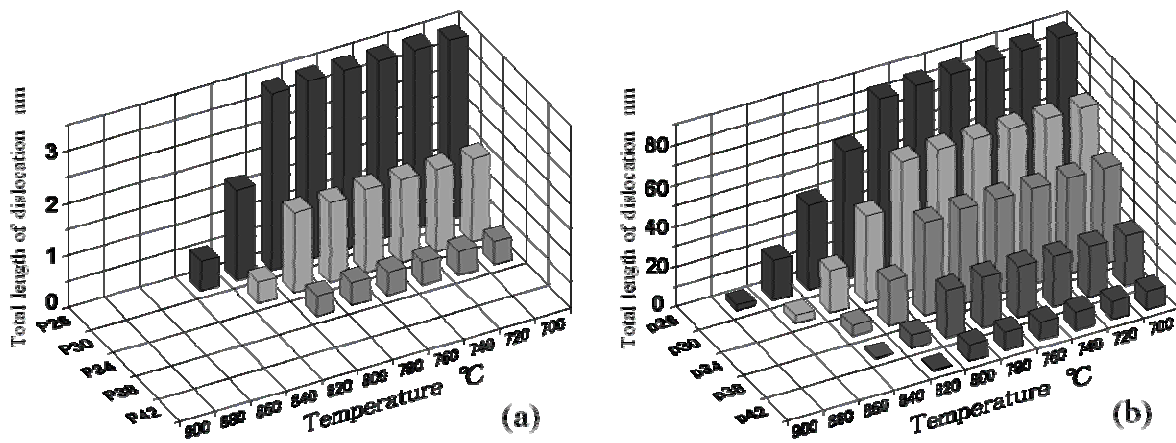


Fig. 2 Total length of dislocations during cooling on (a) $(111)[\bar{1}\bar{1}0]$ slip system and (b) $(11\bar{1})[\bar{1}\bar{1}0]$ slip system.

Fig. 3 (a) and (b) show numerical results for the density distribution of the geometrically necessary dislocations on the $(111)[\bar{1}\bar{1}0]$ and $(11\bar{1})[\bar{1}\bar{1}0]$ slip systems at 780 , when the lattice friction stress is given by P34 and P26. Direction of line segments is parallel to the dislocation line. Longer and thicker line segments represent higher density of dislocations. $\|\rho_G\|_{\max}$ is the maximum dislocation density in the device. Dislocations accumulated on the $(111)[\bar{1}\bar{1}0]$ slip system and shown in Fig. 3 (a) are mostly straight and lie parallel to the trench direction at the bottom corner of the trench. Dislocations accumulated on the $(111)[10\bar{1}]$, $(\bar{1}11)[110]$ and $(\bar{1}11)[101]$ systems also make up a similar structure as the one shown in Fig. 3 (a). When the lattice friction stress is given by P26, the maximum dislocation density is 3.8 times larger than the one obtained for P34 case.

Dislocations shown in Fig. 3 (b) make up half loop shaped structures at bottom corners of the trench. Dislocations on the $(11\bar{1})[101]$, $(1\bar{1}1)[110]$ and $(1\bar{1}1)[10\bar{1}]$ slip systems also make up a similar structure as the one given in Fig. 3 (b). When the lattice friction stress is given by P26,

dislocations make up half loop shaped structure also at the shoulder part of the device area. The shoulder part serves as a part of electron channel and dislocations there will cause fatal damages for normal operation of devices. While, impurity atoms are usually introduced into the electron channel and this will cause alteration of lattice friction stress. Such effects on the thermo-plastic deformation in STI structure are left to be studied.

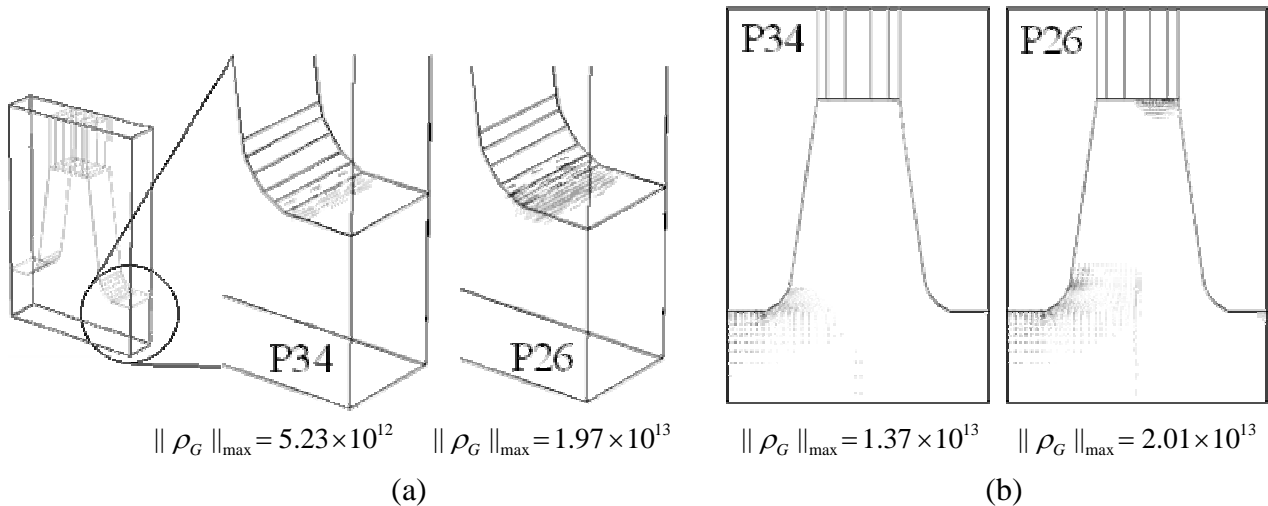


Fig. 3 Structures of GN dislocations (a) on the $(111)[\bar{1}10]$ slip system, and (b) on the $(11\bar{1})[\bar{1}10]$ slip system, when the temperature is 780 .

Summary

We analyzed thermo-plastic deformation and dislocation accumulation with consideration of temperature dependence of the lattice friction stress in the periodic structure of shallow trench isolation (STI) type ULSI cells when the temperature drops from 1000 to room temperature. Results are summarized as follows;

- (1) Dislocation accumulation started from 880 to 800 and converged at 800 when the temperature dependency of lattice friction stress was considered.
- (2) Two types of structure of dislocations were generated; one at the shoulder part of the device area and the other at bottom corners of the trench when the temperature dropped.
- (3) Difference of less than 20 MPa in the lattice friction stress at the temperature range from 1000 to 800 made a significant changes in the final structure of dislocation accumulations.

References

- [1] Ohashi, T., *Phil. Mag. Lett.*, 75(1997), 51.
- [2] Ohashi, T., *Int. J. Plasticity*, 21(2005), 2071.
- [3] *Semiconductors Handbook*, revised ed., edited by Semiconductors Handbook Compilation Committee, Ohm-sha Publishing, Tokyo, 1977, p. 135.
- [4] *Encyclopedia for Physics and Chemistry*, 3rd ed., edited by B. Tamamushi, Iwanami Publishing, Tokyo, 1981, pp. 1068, 1151.
- [5] Ashby, M.F., *Phil. Mag.*, 21(1970), 399.
- [6] Ohashi, T., *J. Mater. Res.*, 7(1992), 3032.
- [7] Properties of Silicon, EMIS DATA REVIEWS SERIES No.4, AHMED, H., INSPEC, (1988), 22.